

## GILDED MEDIEVAL ISLAMIC GLAZED CERAMICS: PRODUCTION PROCESS AND EVOLUTION IN THE IRANIAN WORLD (12<sup>TH</sup>-13<sup>TH</sup> C.) AND THE TIMURID EMPIRE (14<sup>TH</sup>-15<sup>TH</sup> C.)

<sup>1</sup>C. Pacheco – <sup>2</sup>R. CHAPOULIE – <sup>3</sup>E. DOORYHEE – <sup>4</sup>M. AUCOUTURIER – <sup>4</sup>A. BOUQUILLON – <sup>5</sup>S. MAKARIOU – <sup>5</sup>D. MIROUDOT

<sup>1</sup>ENSMP – CEMEF – SET group, [claire.pacheco@ensmp.fr](mailto:claire.pacheco@ensmp.fr)

<sup>2</sup>IRAMAT-CRP2A UMR 5060 CNRS/Université Bordeaux 3, Maison de l'archéologie  
[remy.chapoulie@u-bordeaux3.fr](mailto:remy.chapoulie@u-bordeaux3.fr)

<sup>3</sup>Institut Néel – MCMF – CNRS/Université Joseph Fourier, [eric.dooryhee@grenoble.cnrs.fr](mailto:eric.dooryhee@grenoble.cnrs.fr)

<sup>4</sup>C2RMF – UMR 171 – CNRS/Ministère de la Culture  
[marc.aucouturier@culture.gouv.fr](mailto:marc.aucouturier@culture.gouv.fr); [anne.bouquillon@culture.gouv.fr](mailto:anne.bouquillon@culture.gouv.fr)

<sup>5</sup>Département des Arts de l'Islam – Musée du Louvre  
[sophie.makariou@louvre.fr](mailto:sophie.makariou@louvre.fr); [delphine.miroudot@louvre.fr](mailto:delphine.miroudot@louvre.fr)

**Abstract:** *The main steps of the production process of gold-leaf decoration applied on medieval Islamic glazed ceramics have been determined. Non-destructive analyses have been privileged as SEM-EDS and PIXE to determine the chemical compositions of the ceramic body, the glaze and the metal. RBS enables to estimate the thickness of the gold leaf. Surface XRD pole figures give information on the mechanical treatment the gold leaf underwent. The comparison of Timurid tiles (14<sup>th</sup>-15<sup>th</sup> c., Central Asia) with 12<sup>th</sup>-13<sup>th</sup>-c. Iranian sherds and Abu'l Qasim's Treatise on Ceramics (1301) enables to conclude that the making process was similar but the interaction between the potters and gold beaters' crafts societies were different in the two geo-chronological contexts.*

**Keywords:** *Medieval Islamic glazed ceramics, gold leaf, production process, XRD pole figures, RBS.*

### INTRODUCTION

A society can be described by a social, political, religious and economical structure in which objects made of synthetic materials, such as metal, glass and ceramics are produced according to specific techniques. The evolution of the latter is representative of the very change of the society itself. The technique can be described by a *chaîne opératoire* as suggested by *Leroi-Gourhan (1945)* composed by the materials, the tools, the gestures and the knowledge. Materials and tools are physical archaeological remains but gestures and knowledge belong to an intangible heritage. The laboratory study of the archaeological sherds enables not only to study the material itself but also to find out some technological features which are the consequences of specific gestures (*Pernot 2006*).

This study is dedicated to Islamic glazed ceramics decorated with gold leaves. The first question is: what were the interactions between the potters' and the gold beaters' craft societies? Then, is this type of decoration commonly used in 14<sup>th</sup>-15<sup>th</sup>-c. Central Asia a Persian tradition is the same kind of decorations that was made in 12<sup>th</sup>-13<sup>th</sup> c. Iran?

The aims are to study two corpuses of gilded samples coming from the latter geo-chronological contexts in order to determine the main steps of the *chaîne opératoire* of their making and then to compare them. A methodology adapted to these peculiar objects had to be

developed, privileging non-destructive observation and analytical techniques.

### EXPERIMENTAL PROCEDURE

#### *Studied material*

The studied material is composed, on the one hand, by 25 Timurid sherds coming from the collections of the Amir Timur Museum in Shahrisabz (Uzbekistan), hometown of Timur (1336-1405), and more precisely from excavations of his *Aq Saray* palace, built between 1380 and 1405, and of the *Dorus-Siadat* and *Dorut-Tilovat* complexes built in the 15<sup>th</sup> c. by Tamerlane's heirs (*Blair & Bloom 1994*). As Timurid glazed ceramic is considered as a *Persian tradition* (*Kehren 1978; Porter 1995*), a 33-Iranian-fragment corpus of 12<sup>th</sup>-13<sup>th</sup> c. Iranian gilded sherds has been constituted from the collections of the Islamic Art Department of the Louvre Museum.

#### *Surface observations*

The surface was observed with different magnification devices: a binocular magnifier WILD MSA Heerbrugg, an Olympus BX60 microscope and a JEOL JSM6460LV scanning electron microscope (SEM) in secondary electron (SE) and backscattered electron (BSE) modes. The purpose was to determine the organisation and the surface state of the decorations.

**Table 1** Chemical composition of the ceramic bodies determined by SEM-EDS. The results are given with a 1- $\sigma$  standard deviation. Two groups can be distinguished: ferruginous calcareous earthenwares and stonewares (high lighted in grey).

Sample	Na <sub>2</sub> O	MgO	Al <sub>2</sub> O <sub>3</sub>	SiO <sub>2</sub>	P <sub>2</sub> O <sub>5</sub>	SO <sub>3</sub>	K <sub>2</sub> O	CaO	TiO <sub>2</sub>	Fe <sub>2</sub> O <sub>3</sub>
BDX 6301	1.3 ± 0.2	1.5 ± 0.1	3.3 ± 0.7	86.3 ± 1.9	-	-	0.9 ± 0.1	5.2 ± 1	-	1.0 ± 0.1
BDX 6303	1.6 ± 0.1	2.8 ± 0.2	12.4 ± 0.6	58.6 ± 2.2	0.5 ± 0.1	0.3 ± 0.1	2.8 ± 0.2	14.1 ± 2.2	0.6 ± 0.1	6.4 ± 0.5
BDX 6316	2.3 ± 0.2	5.3 ± 0.4	14.5 ± 0.6	56.7 ± 1.8	0.4 ± 0.2	-	1.3 ± 0.2	14.0 ± 1.1	0.5 ± 0.1	5.1 ± 0.7
BDX 6317	2.7 ± 0.7	3.0 ± 0.2	12.2 ± 0.6	61.3 ± 1.3	0.6 ± 0.2	-	2.1 ± 0.2	11.7 ± 1.0	0.6 ± 0.1	5.8 ± 0.5
BDX 8019	1.5 ± 0.1	3.6 ± 0.3	11.7 ± 0.5	55.4 ± 1.1	-	-	2.1 ± 0.3	18.1 ± 1.0	0.6 ± 0.1	6.9 ± 0.8
BDX 8022	2.4 ± 0.2	2.5 ± 0.3	5.2 ± 0.4	79.6 ± 1.3	0.5 ± 0.1	-	-	2.0 ± 0.1	4.6 ± 0.4	0.3 ± 0.1
BDX 8023	1.6 ± 0.1	3.7 ± 0.2	11.7 ± 0.3	51.3 ± 1.2	-	-	2.0 ± 0.2	20.7 ± 1.2	0.7 ± 0.1	7.9 ± 0.5
BDX 8025	1.6 ± 0.2	2.9 ± 0.2	12.2 ± 0.6	59.6 ± 1.3	0.3 ± 0.1	-	3.0 ± 0.2	13.1 ± 1.0	0.7 ± 0.2	6.6 ± 0.5
BDX 8039	2.0 ± 0.4	2.8 ± 0.6	11.7 ± 2.3	56.5 ± 6.4	0.5 ± 0.2	0.4 ± 0.2	2.1 ± 0.8	18.1 ± 2.5	0.6 ± 0.4	5.2 ± 1.0
BDX 8044	2.2 ± 0.2	3.0 ± 0.1	12.5 ± 0.6	56.7 ± 1.2	0.3 ± 0.2	0.3 ± 0.1	2.4 ± 0.3	14.5 ± 1.0	0.7 ± 0.1	7.6 ± 0.4
BDX 8046	1.6 ± 0.2	3.3 ± 0.2	11.9 ± 0.5	58.7 ± 1.7	0.6 ± 0.1	1.5 ± 0.2	2.9 ± 0.3	13.3 ± 0.9	0.7 ± 0.2	5.3 ± 0.3
BDX 8048	1.6 ± 0.1	3.4 ± 0.2	11.2 ± 0.3	53.7 ± 1.7	-	0.5 ± 0.1	2.7 ± 0.2	19.3 ± 1.6	0.9 ± 0.2	6.6 ± 0.3
BDX 8052	1.5 ± 0.1	3.0 ± 0.1	12.7 ± 0.5	55.6 ± 0.9	0.3 ± 0.2	-	2.6 ± 0.2	15.7 ± 0.8	0.8 ± 0.2	7.8 ± 0.3
BDX 8057	1.4 ± 0.3	1.2 ± 0.2	3.5 ± 0.8	87.2 ± 2.3	0.3 ± 0.1	0.3 ± 0.1	1.5 ± 0.3	3.1 ± 0.5	-	1.2 ± 0.5
BDX 8058	2.7 ± 0.2	7.5 ± 0.5	16.9 ± 0.8	59.1 ± 0.8	-	-	0.9 ± 0.2	12.4 ± 1.6	-	5.2 ± 0.2
BDX 8062	2.4 ± 0.7	3.0 ± 0.2	11.1 ± 0.6	53.1 ± 2.9	0.3 ± 0.1	0.4 ± 0.1	1.7 ± 0.2	20.6 ± 3.2	0.6 ± 0.1	6.8 ± 0.8
BDX 8063	1.8 ± 0.2	3.0 ± 0.2	10.8 ± 0.3	57.8 ± 1.8	0.4 ± 0.1	0.5 ± 0.1	2.6 ± 0.2	17.0 ± 1.7	0.7 ± 0.1	5.5 ± 0.3
BDX 8065	1.5 ± 0.1	3.0 ± 0.2	12.6 ± 0.6	59.3 ± 2.1	0.3 ± 0.1	-	3.1 ± 0.3	12.7 ± 1.4	0.8 ± 0.2	6.6 ± 0.5
BDX 8070	1.5 ± 0.3	3.9 ± 0.5	12.2 ± 0.7	55.0 ± 2.1	0.6 ± 0.2	0.4 ± 0.1	2.8 ± 0.3	17.6 ± 1.5	0.6 ± 0.2	5.5 ± 0.4
BDX 8075	1.2 ± 0.2	3.1 ± 0.4	12.9 ± 1.1	55.5 ± 3.1	0.4 ± 0.1	0.5 ± 0.1	2.7 ± 0.3	16.1 ± 1.0	0.7 ± 0.1	6.9 ± 0.5
BDX 8078	1.2 ± 0.5	1.3 ± 0.3	2.9 ± 0.2	87.3 ± 2.3	0.3 ± 0.1	-	0.4 ± 0.1	5.8 ± 1.0	-	0.8 ± 0.6
MAO 449-47	3.8 ± 0.4	0.6 ± 0.2	9.8 ± 1.4	80.9 ± 2.2	0.4 ± 0.1	0.5 ± 0.1	1.3 ± 0.3	1.3 ± 0.3	0.6 ± 0.1	0.7 ± 0.1
MAO 449-50	3.3 ± 0.5	0.7 ± 0.3	4.9 ± 0.8	86.5 ± 2.1	0.3 ± 0.1	0.3 ± 0.0	1.1 ± 0.2	1.3 ± 0.4	0.8 ± 0.2	0.7 ± 0.2
MAO 489-56	3.1 ± 0.6	0.7 ± 0.2	5.0 ± 1.3	86.6 ± 3.1	-	0.3 ± 0.2	0.8 ± 0.1	1.7 ± 0.5	0.8 ± 0.2	0.8 ± 0.2
MAO 489-77	5.0 ± 0.6	1.0 ± 0.3	9.3 ± 1.4	79.8 ± 2.3	0.2 ± 0.2	0.4 ± 0.1	1.6 ± 0.2	1.4 ± 0.3	0.6 ± 0.2	0.6 ± 0.3
MAO 489-107	3.9 ± 0.3	0.6 ± 0.2	8.1 ± 0.8	82.9 ± 1.3	0.2 ± 0.1	0.4 ± 0.1	1.5 ± 0.1	1.0 ± 0.3	0.9 ± 0.6	0.4 ± 0.1
MAO 489-108	3.6 ± 0.4	1.1 ± 0.4	8.5 ± 1.1	80.2 ± 2.3	0.4 ± 0.2	0.4 ± 0.1	2.2 ± 0.3	1.9 ± 0.7	0.8 ± 0.3	0.9 ± 0.2
MAO 489-113	4.2 ± 0.3	0.7 ± 0.2	8.9 ± 1.0	80.9 ± 1.5	-	-	1.7 ± 0.1	1.4 ± 0.4	0.9 ± 0.3	0.7 ± 0.2
MAO 489-114	4.1 ± 0.9	1.0 ± 0.7	9.1 ± 2.4	79.2 ± 5.0	0.4 ± 0.1	0.5 ± 0.1	1.4 ± 0.3	2.4 ± 1.3	0.6 ± 0.2	1.2 ± 0.6
MAO 936-277	3.6 ± 0.7	0.7 ± 0.3	7.1 ± 1.5	83.8 ± 2.9	0.3 ± 0.2	0.2 ± 0.1	1.3 ± 0.2	1.6 ± 0.6	0.6 ± 0.2	0.6 ± 0.1
MAO 936-323	4.3 ± 0.5	0.9 ± 0.2	8.9 ± 1.5	79.9 ± 2.0	0.3 ± 0.1	0.3 ± 0.0	2.0 ± 0.2	1.7 ± 0.3	1.0 ± 0.3	0.6 ± 0.1
MAO 936-331	4.2 ± 1.2	0.8 ± 0.3	6.9 ± 1.9	82.7 ± 5.7	0.6 ± 0.3	0.5 ± 0.1	1.2 ± 0.3	1.2 ± 0.7	1.0 ± 0.8	0.7 ± 0.5
MAO 936-333	3.9 ± 0.6	0.8 ± 0.2	8.2 ± 1.5	81.5 ± 2.4	0.5 ± 0.1	0.4 ± 0.1	1.3 ± 0.2	1.7 ± 0.3	0.9 ± 0.2	0.6 ± 0.1

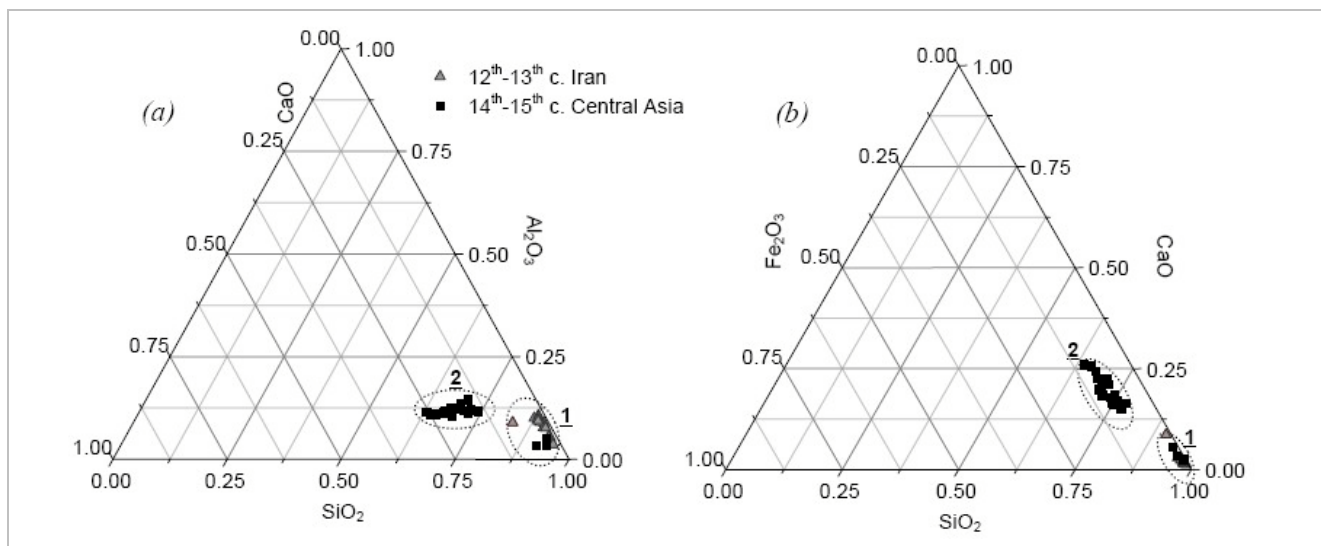


**Fig. 1** Chemical compositions of the ceramic bodies represented in ternary diagrams SiO<sub>2</sub>-Al<sub>2</sub>O<sub>3</sub>-CaO (a) and SiO<sub>2</sub>-CaO-Fe<sub>2</sub>O<sub>3</sub> (b). Two groups can be distinguished: the first one is rich in silica and is characteristic of stonewares; the second one is representative of ferruginous, calcareous earthenwares.

**Table 2** Chemical compositions of the glazes determined by SEM-EDS. The results are given with a 1-σ standard deviation. The different colours of the glazes are white, turquoise blue (high lighted in light grey) and dark blue (high lighted in dark grey).

	Na <sub>2</sub> O	MgO	Al <sub>2</sub> O <sub>3</sub>	SiO <sub>2</sub>	Cl	K <sub>2</sub> O	CaO	Fe <sub>2</sub> O <sub>3</sub>	SnO <sub>2</sub>	PbO	CoO	CuO	As <sub>2</sub> O <sub>3</sub>	Cr <sub>2</sub> O <sub>3</sub>
14 <sup>th</sup> -15 <sup>th</sup> -c. Central Asia	BDX6301	8.2 ± 0.1	2.7 ± 0.1	2.1 ± 0.1	53.6 ± 1.5	0.3 ± 0.1	1.3 ± 0.1	4.4 ± 0.1	0.9 ± 0.1	11.1 ± 1.4	15.1 ± 0.3	-	-	-
	BDX 6303	9.8 ± 0.1	2.8 ± 0.1	1.4 ± 0.2	58.3 ± 0.5	0.7 ± 0.1	2.6 ± 0.1	5.8 ± 0.2	0.7 ± 0.1	6.0 ± 0.5	11.4 ± 0.4	-	-	-
	BDX 6316	12.0 ± 0.5	3.4 ± 0.2	1.2 ± 0.2	56.5 ± 0.5	0.6 ± 0.2	2.6 ± 0.1	3.2 ± 0.1	0.3 ± 0.1	4.1 ± 0.3	15.8 ± 0.5	-	-	-
	BDX 6317	7.9 ± 0.1	2.8 ± 0.1	2.6 ± 0.2	55.7 ± 1.0	-	2.5 ± 0.1	6.2 ± 0.2	0.9 ± 0.1	7.2 ± 1.5	13.8 ± 0.3	-	-	-
	BDX 8019	10.6 ± 0.2	2.9 ± 0.1	2.1 ± 0.4	51.8 ± 1.0	0.7 ± 0.1	3.1 ± 0.2	4.7 ± 0.3	0.7 ± 0.2	6.9 ± 1.8	16.4 ± 0.7	-	-	-
	BDX 8022	14.9 ± 0.2	3.7 ± 0.1	1.7 ± 0.1	69.1 ± 0.7	0.6 ± 0.1	1.9 ± 0.1	4.4 ± 0.1	2.5 ± 0.5	0.2 ± 0.1	-	0.4 ± 0.1	-	-
	BDX 8023	9.9 ± 0.2	3.0 ± 0.1	2.6 ± 0.1	53.2 ± 0.6	0.4 ± 0.1	2.8 ± 0.1	5.8 ± 0.1	1.1 ± 0.1	7.0 ± 1.0	14.0 ± 0.2	-	-	-
	BDX 8025	14.4 ± 0.4	1.1 ± 0.1	2.2 ± 0.1	55.6 ± 0.4	0.9 ± 0.1	2.8 ± 0.1	4.4 ± 0.2	4.0 ± 0.2	1.7 ± 0.2	12.9 ± 0.6	-	-	-
	BDX 8039	8.0 ± 0.1	2.1 ± 0.1	2.7 ± 0.4	52.2 ± 0.7	0.4 ± 0.1	2.1 ± 0.1	4.7 ± 0.3	1.0 ± 0.1	7.4 ± 1.1	19.1 ± 1.2	-	-	-
	BDX 8044	10.5 ± 0.3	2.6 ± 0.2	2.1 ± 1.3	56.3 ± 1.2	0.5 ± 0.1	1.9 ± 0.2	4.7 ± 0.5	0.8 ± 0.4	8.4 ± 1.8	11.8 ± 1.1	-	-	-
	BDX 8046	7.6 ± 0.1	2.4 ± 0.1	1.8 ± 0.2	59.1 ± 0.9	-	3.6 ± 0.1	4.1 ± 0.3	0.6 ± 0.1	5.6 ± 0.3	14.7 ± 0.6	-	-	-
	BDX 8048	11.7 ± 0.2	2.5 ± 0.2	1.0 ± 0.1	51.9 ± 0.7	0.7 ± 0.1	1.4 ± 0.1	3.6 ± 0.5	0.4 ± 0.1	7.5 ± 1.1	19.3 ± 0.3	-	-	-
	BDX 8052	1.4 ± 0.1	2.6 ± 0.1	1.4 ± 0.1	57.9 ± 0.3	0.6 ± 0.1	2.1 ± 0.1	4.8 ± 0.2	0.7 ± 0.1	6.0 ± 0.1	13.3 ± 0.4	-	-	-
	BDX 8057	11.2 ± 0.2	3.3 ± 0.2	2.3 ± 0.6	70.4 ± 1.0	0.5 ± 0.1	2.4 ± 0.1	4.9 ± 0.3	3.6 ± 0.3	0.3 ± 0.1	-	0.5 ± 0.1	-	-
	BDX 8058	9.5 ± 0.3	3.3 ± 0.1	2.1 ± 0.1	56.7 ± 0.5	0.4 ± 0.1	2.7 ± 0.1	5.8 ± 0.1	0.6 ± 0.1	6.1 ± 0.6	12.8 ± 0.5	-	-	-
	BDX 8062	8.3 ± 0.1	2.3 ± 0.1	2.8 ± 0.2	52.4 ± 0.3	0.4 ± 0.1	3.2 ± 0.1	5.8 ± 0.3	1.1 ± 0.1	6.8 ± 0.8	16.6 ± 1.3	-	-	-
	BDX 8063	10.1 ± 0.1	3.1 ± 0.1	1.7 ± 0.1	57.0 ± 0.4	0.7 ± 0.1	2.2 ± 0.1	5.7 ± 0.1	0.7 ± 0.1	6.3 ± 0.6	12.3 ± 0.4	-	-	-
	BDX 8065	9.6 ± 0.1	2.3 ± 0.1	2.3 ± 0.1	56.6 ± 0.5	0.5 ± 0.1	2.3 ± 0.1	4.7 ± 0.2	1.1 ± 0.1	5.8 ± 0.6	14.4 ± 0.4	-	-	-
	BDX 8070	10.4 ± 0.3	2.0 ± 0.2	1.8 ± 0.6	54.6 ± 3.5	0.6 ± 0.1	2.4 ± 0.2	3.2 ± 0.2	0.8 ± 0.2	8.0 ± 1.9	16.0 ± 0.9	-	-	-
	BDX 8075	7.8 ± 0.1	1.5 ± 0.1	1.6 ± 0.3	54.0 ± 0.9	0.5 ± 0.1	2.5 ± 0.1	3.6 ± 0.6	0.8 ± 0.1	6.7 ± 1.0	20.8 ± 1.2	-	-	-
BDX 8078	8.8 ± 0.1	2.5 ± 0.1	2.3 ± 0.2	63.6 ± 0.4	-	2.7 ± 0.1	4.9 ± 0.1	0.7 ± 0.1	5.2 ± 0.6	8.8 ± 0.5	-	-	-	
12 <sup>th</sup> -13 <sup>th</sup> -c. Iran	MAO 449-37	11.5 ± 0.2	3.1 ± 0.1	1.3 ± 0.1	65.1 ± 0.4	0.3 ± 0.1	2.2 ± 0.1	4.8 ± 0.1	1.2 ± 0.1	2.6 ± 0.2	6.3 ± 0.1	0.6 ± 0.1	0.4 ± 0.1	0.6 ± 0.1
	MAO 449-43	7.3 ± 0.1	1.6 ± 0.1	2.3 ± 0.6	57.7 ± 0.8	0.5 ± 0.1	1.3 ± 0.1	3.6 ± 0.3	0.8 ± 0.1	6.6 ± 1.0	18.1 ± 1.1	-	-	-
	MAO 449-47	7.1 ± 0.1	1.4 ± 0.1	1.3 ± 0.1	52.1 ± 0.6	0.6 ± 0.1	1.1 ± 0.1	2.7 ± 0.1	0.3 ± 0.1	7.8 ± 0.9	24.2 ± 0.2	-	1.4 ± 0.1	-
	MAO 449-50	8.0 ± 0.3	1.9 ± 0.1	1.4 ± 0.1	53.7 ± 3.0	0.6 ± 0.1	1.2 ± 0.1	2.9 ± 0.2	0.6 ± 0.1	7.7 ± 4.9	20.7 ± 1.1	-	1.0 ± 0.1	-
	MAO 449-527	8.7 ± 0.1	2.1 ± 0.1	1.6 ± 0.1	55.4 ± 0.6	0.8 ± 0.1	2.4 ± 0.1	3.6 ± 0.1	1.8 ± 0.1	5.0 ± 0.4	17.4 ± 0.3	-	2.0 ± 0.1	-
	MAO 449-575	14.5 ± 0.2	3.6 ± 0.1	1.6 ± 0.1	68.0 ± 0.3	0.6 ± 0.1	3.0 ± 0.1	5.4 ± 0.1	1.3 ± 0.1	-	-	0.6 ± 0.1	-	0.6 ± 0.1
	MAO 489-56	6.8 ± 0.2	1.5 ± 0.1	1.1 ± 0.1	52.8 ± 1.0	0.3 ± 0.1	0.9 ± 0.1	2.8 ± 0.1	0.7 ± 0.1	7.5 ± 1.3	25.4 ± 0.8	-	-	-
	MAO 489-64	6.5 ± 0.1	1.5 ± 0.1	1.8 ± 0.4	54.6 ± 1.4	0.5 ± 0.1	1.3 ± 0.2	2.9 ± 0.2	4.6 ± 0.6	5.9 ± 1.1	18.6 ± 0.5	-	-	1.4 ± 0.1
	MAO 489-77	7.3 ± 0.1	1.9 ± 0.1	1.3 ± 0.1	50.6 ± 1.4	0.6 ± 0.1	1.4 ± 0.1	2.8 ± 0.1	0.6 ± 0.2	8.3 ± 2.2	25.2 ± 0.7	-	-	-
	MAO 489-84	6.7 ± 0.1	1.2 ± 0.1	1.5 ± 0.2	53.0 ± 0.8	0.7 ± 0.1	1.4 ± 0.1	2.5 ± 0.1	0.7 ± 0.1	7.3 ± 1.2	24.8 ± 0.5	-	-	-
	MAO 489-107	7.6 ± 0.2	1.9 ± 0.1	1.5 ± 0.1	54.1 ± 1.2	0.5 ± 0.1	1.4 ± 0.1	3.2 ± 0.1	0.5 ± 0.1	8.0 ± 1.8	21.2 ± 0.4	-	-	-
	MAO 489-108	7.9 ± 0.1	1.8 ± 0.1	2.5 ± 0.4	55.5 ± 1.1	0.5 ± 0.1	2.2 ± 0.1	3.8 ± 0.3	0.8 ± 0.1	5.6 ± 0.8	17.6 ± 0.9	-	1.5 ± 0.2	-
	MAO 489-113	6.6 ± 0.5	1.5 ± 0.1	1.3 ± 0.1	50.9 ± 1.7	0.5 ± 0.1	1.0 ± 0.1	2.7 ± 0.2	0.6 ± 0.1	9.1 ± 2.9	25.6 ± 0.9	-	-	-
	MAO 489-114	6.1 ± 0.1	1.8 ± 0.1	1.5 ± 0.1	55.7 ± 1.5	0.3 ± 0.1	1.0 ± 0.1	3.2 ± 0.1	0.6 ± 0.1	6.4 ± 2.2	21.8 ± 0.5	-	1.6 ± 0.1	-
	MAO 936-277	7.1 ± 0.1	1.8 ± 0.1	1.6 ± 0.1	54.9 ± 0.8	0.2 ± 0.1	1.1 ± 0.1	3.8 ± 0.1	0.8 ± 0.1	6.5 ± 1.2	20.4 ± 0.4	-	1.6 ± 0.1	-
	MAO 936-323	7.4 ± 0.1	1.9 ± 0.1	2.2 ± 0.1	56.1 ± 1.1	0.3 ± 0.1	1.7 ± 0.1	5.0 ± 0.1	0.8 ± 0.1	8.6 ± 1.7	15.7 ± 0.4	-	-	-
	MAO 936-331	7.2 ± 0.1	1.6 ± 0.1	1.3 ± 0.1	54.6 ± 0.5	0.4 ± 0.1	1.2 ± 0.1	2.6 ± 0.1	0.4 ± 0.1	6.6 ± 0.9	24.1 ± 0.4	-	-	-
	MAO 936-332	7.5 ± 0.1	1.7 ± 0.1	1.4 ± 0.1	52.1 ± 0.7	0.7 ± 0.1	1.1 ± 0.1	2.7 ± 0.1	0.5 ± 0.1	6.8 ± 1.2	25.1 ± 0.7	-	-	-
	MAO 936-333	6.6 ± 0.2	1.9 ± 0.1	1.7 ± 0.2	53.7 ± 1.5	0.3 ± 0.1	1.2 ± 0.1	3.5 ± 0.2	0.7 ± 0.1	8.0 ± 2.0	22.2 ± 1.1	-	-	-

**Table 3** Chemical compositions of Iranian sherds determined by PIXE under a 3-MeV proton beam. The different colours of the glazes are white, turquoise blue (high lighted in light grey) and dark blue (high lighted in dark grey). The values in brackets are given as an indication: although they are above the detection threshold, they are inferior to the quantification one.

	SiO <sub>2</sub>	Na <sub>2</sub> O	K <sub>2</sub> O	PbO	Al <sub>2</sub> O <sub>3</sub>	CaO	MgO	Fe <sub>2</sub> O <sub>3</sub>	CuO	SnO <sub>2</sub>	P <sub>2</sub> O <sub>5</sub>	Cl	TiO <sub>2</sub>	Cr <sub>2</sub> O <sub>3</sub>	MnO	CoO	NiO	Zn	As <sub>2</sub> O <sub>3</sub>	SrO	Total
MAO 449-527	55.9	1.0	3.1	9.0	5.2	2.7	2.1	1.5	1.7	8.9	53809	1138	2236	-	283	(71)	(20)	333	-	544	97.0
MAO 489-105	50.5	6.4	1.5	16.3	3.0	5.8	2.0	2.1	0.2	6.8	16087	(936)	1053	3654	1560	33195	(256)	225	27323	514	103.1
MAO 489-105	55.2	7.5	1.4	14.0	3.3	3.9	1.8	5.7	1.2	6.2	(3742)	(1334)	1115	907	432	(550)	(53)	207	1592	399	101.2
MAO 489-113	46.8	2.1	3.8	13.6	3.6	1.4	1.2	1.0	0.1	11.3	15490	17917	2262	-	251	(102)	55	196	(59)	299	88.6
MAO 489-114	50.8	4.4	1.0	24.1	2.0	4.2	3.1	0.8	2.8	6.0	-	3092	991	-	536	(123)	(58)	255	(85)	874	99.8
MAO 573	55.1	5.9	2.3	15.8	2.1	2.3	1.6	0.6	0.1	9.7	(4280)	3050	1251	-	341	(189)	95	158	(372)	424	96.6
MAO 936-277	45.07	1.9	2.0	17.7	1.9	6.2	4.0	1.2	1.8	11.3	26043	5853	2893	-	540	(150)	103	343	-	583	96.8
MAO 936-285	53.6	0.3	1.4	18.0	5.1	4.1	0.2	1.2	0.1	7.2	5455	1080	2475	-	529	2090	95	134	2214	590	92.8
MAO 936-322	46.0	3.7	1.0	23.2	2.9	6.1	3.3	2.0	2.3	8.8	(7403)	3539	1697	(687)	740	(204)	145	191	970	855	101.0
MAO 936-323	60.0	6.9	1.5	13.8	1.5	2.2	1.7	0.9	0.7	9.7	-	1199	1225	-	359	432	59	442	607	567	99.3
MAO 936-323	61.0	6.3	1.8	12.6	2.5	2.8	1.2	0.8	0.2	9.4	-	(859)	1540	(123)	262	(80)	48	142	(100)	669	99.2
MAO 936-323	59.2	6.4	1.9	14.2	3.0	3.5	1.9	1.3	0.1	7.1	(2556)	1295	1471	-	467	7333	120	195	5587	660	100.6
MAO 2058	55.6	3.7	1.6	19.4	1.8	2.8	2.5	0.6	2.7	8.9	(3945)	2489	656	-	332	(78)	73	309	(449)	325	100.4

*An ancient text considered as scientific data*

Abu'l Qasim al-Kashani wrote a Treatise on Mineralogy in 1301 (*Allan 1973*). As a heir of a traditional potter family a part of his works is dedicated to ceramic techniques and a chapter deals specially with gilded glazed objects. The text has to be translated into materials science language in order to compare the medieval recipe with the surface observations made on the ancient sherds.

*Chemical compositions*

The chemical compositions of the ceramic substrates, the glazes and the gold decorations were determined by X-ray energy dispersive spectroscopy (EDS) with a Si(Li) detector attached to the previously mentioned SEM. Polished cross-sections were used for the ceramic bodies and the glazes whereas the gold decorations were analysed on the surface. Some glazes were non-destructively studied with PIXE at the AGLAE facility under a 3-MeV proton beam.

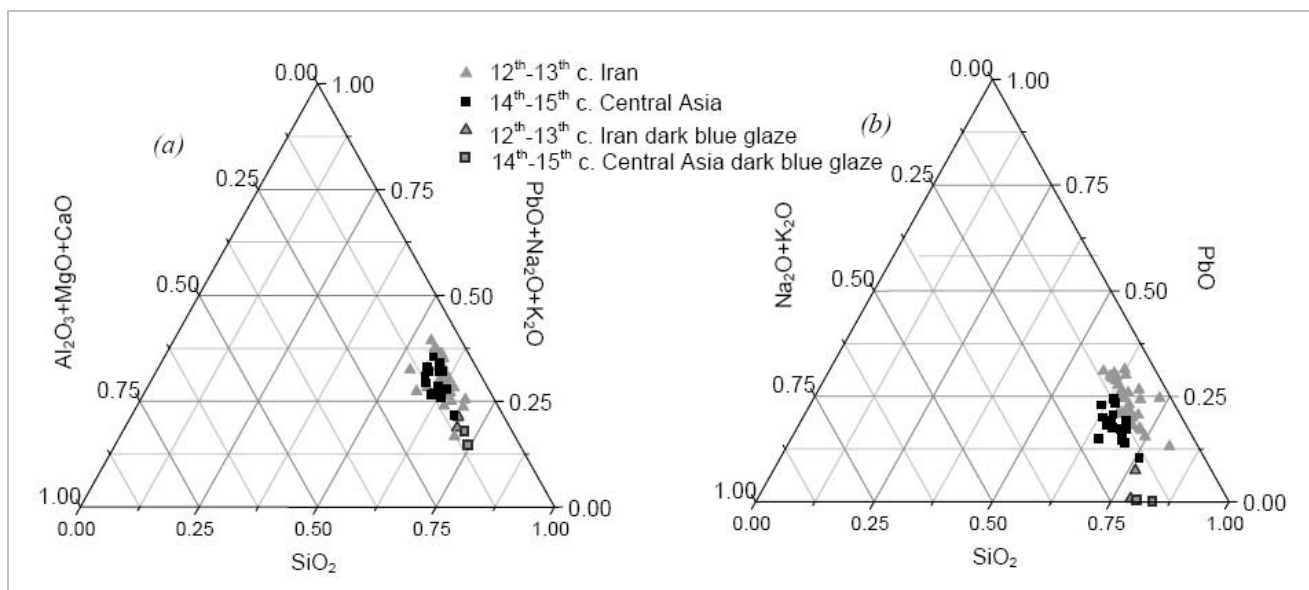


**Fig. 2** Chemical compositions of the glazes represented in ternary diagrams SiO<sub>2</sub>-(PbO+Na<sub>2</sub>O+K<sub>2</sub>O)-(Al<sub>2</sub>O<sub>3</sub>+MgO+CaO) (a) and SiO<sub>2</sub>-PbO-(Na<sub>2</sub>O+K<sub>2</sub>O) (b). The first one represents the silica ratios as a function of fluxes (PbO+Na<sub>2</sub>O+K<sub>2</sub>O) and of stabilizers (Al<sub>2</sub>O<sub>3</sub>+MgO+CaO). The second one reveals the alkali-lead character of the glazes.

#### *Crystallographic texture of the gold leaf*

X-Ray Diffraction (XRD) pole figures of the gold decoration are determined with a 4-circle diffractometer SIEFERT MZ-VI. They give information on the crystallographic texture of the ancient metal, as derived from the mechanical and thermal treatments carried out on the gold leaf (Pacheco et al. 2007).

#### *Thickness of the gold leaf and gold/glaze interface*

Rutherford Backscattering Spectroscopy (RBS) was considered as an appropriate method to estimate the thickness of the metallic foil and to examine the gold/glaze interface in a non-destructive way. The

experimental spectra are obtained under a 3-MeV proton beam and the simulations are made with the SIMNRA software (Mayer 2006).

## RESULTS AND DISCUSSION

#### *The ceramic bodies*

The results are compiled in **Table 1** and represented in SiO<sub>2</sub>-Al<sub>2</sub>O<sub>3</sub>-CaO and SiO<sub>2</sub>-CaO-Fe<sub>2</sub>O<sub>3</sub> ternary diagrams in **Fig. 1**.

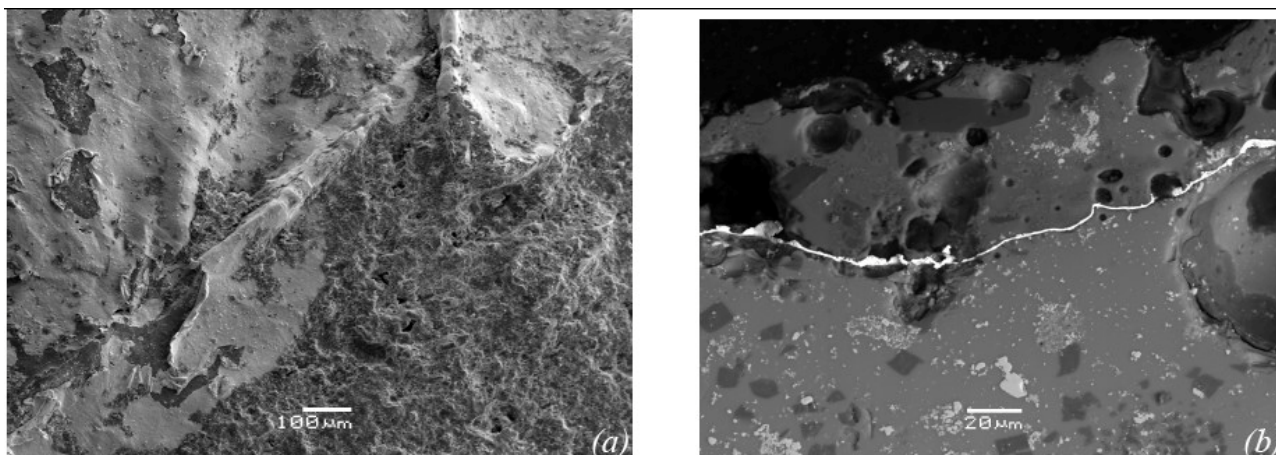


**Fig. 3** Central Asia – 14th-15th c. – SEM images in BSE mode of the surface (a) and a polished cross-section (b) of a gold-leaf decoration covered by a vitreous red decoration

**Table 4** Chemical compositions of the gold leaves determined by SEM-EDS surface analyses. The turquoise-blue glazes are high lighted in grey as part of Cu may belong to the underneath glaze. The results are given with a 1- $\sigma$  standard deviation.

	Sample	Cu	Ag	Au		Sample	Cu	Ag	Au
14 <sup>th</sup> -15 <sup>th</sup> -c. Central Asia	BDX 6301	-	0.9 ± 0.4	99.1 ± 0.4	12 <sup>th</sup> * 13 <sup>th</sup> -c. Iran	MAO 449-37	-	1.5 ± 0.2	98.5 ± 0.2
	BDX 6303	-	0.4 ± 0.2	99.6 ± 0.2		MAO 449-42	-	0.3 ± 0.1	99.7 ± 0.1
	BDX 6316	-	1.1 ± 0.3	98.9 ± 0.3		MAO 449-43	-	-	100.0 ± 0.2
	BDX 6317	-	0.4 ± 0.2	99.6 ± 0.2		MAO 449-47	0.5 ± 0.2	-	99.5 ± 0.2
	BDX 8019	-	0.8 ± 0.2	99.2 ± 0.2		MAO 449-50	-	-	100.0 ± 0.1
	BDX 8022	-	0.7 ± 0.3	99.3 ± 0.3		MAO 449-527	0.4 ± 0.2	0.4 ± 0.1	99.2 ± 0.2
	BDX 8023	-	0.3 ± 0.2	99.7 ± 0.2		MAO 449-575	-	0.5 ± 0.2	99.5 ± 0.2
	BDX 8025	-	0.5 ± 0.2	99.5 ± 0.2		MAO 489-107	-	-	100.0 ± 0.1
	BDX 8039	-	0.4 ± 0.2	99.6 ± 0.2		MAO 489-108	0.5 ± 0.1	-	99.5 ± 0.2
	BDX 8044	-	0.3 ± 0.1	99.7 ± 0.1		MAO 489-113	-	-	100.0 ± 0.1
	BDX 8046	-	0.8 ± 0.2	99.2 ± 0.2		MAO 489-64	0.4 ± 0.2	0.3 ± 0.1	99.3 ± 0.2
	BDX 8048	-	0.6 ± 0.3	99.4 ± 0.3		MAO 489-77	-	-	100.0 ± 0.1
	BDX 8052	-	1.2 ± 0.4	98.8 ± 0.4		MAO 489-84	-	-	100.0 ± 0.2
	BDX 8057	-	0.4 ± 0.2	99.6 ± 0.2		MAO 936-277	2.7 ± 1.3	-	97.3 ± 1.2
	BDX 8058	-	0.6 ± 0.2	99.4 ± 0.2		MAO 936-323	0.3 ± 0.2	-	99.7 ± 0.2
	BDX 8062	-	0.5 ± 0.3	99.5 ± 0.3		MAO 936-331	-	0.3 ± 0.2	99.7 ± 0.2
	BDX 8063	-	0.4 ± 0.1	99.6 ± 0.1		MAO 936-332	-	-	100.0 ± 0.1
	BDX 8065	-	0.8 ± 0.3	99.2 ± 0.3		MAO 936-333	-	-	100.0 ± 0.1
BDX 8070	-	0.6 ± 0.2	99.4 ± 0.2						
BDX 8078	-	3.0 ± 0.4	97.0 ± 0.4						

Two groups can be distinguished: first, high silica containing ceramic bodies, corresponding to stonewares, and then a group made of ferruginous calcareous earthenwares. In 12<sup>th</sup>-13<sup>th</sup> c. Iran only stonewares are used whereas in 14<sup>th</sup>-15<sup>th</sup>-c. Central Asia both substrates are present, earthenwares in a largest way.

In his treatise, Abu'l Qasim only describes how to make stoneware through mixing finely grounded quartz, glass frit and white clay (Allan 1973).

*The glazes*

The chemical compositions of the glazes determined by SEM-EDS are given in Table 2 and by PIXE in Table 3. They are represented in Fig. 2.

As a function of the source of the sherds, the Timurid glazes seem to have more alkali than the Iranian ones. But some PIXE results are not representative of the composition of the wealthy glazes: the analysis is made on the surface which may have been submitted a weathering process as a lixiviation of the alkalis, which resulted in a lower rate in sodium and potassium (Sterpenich & Libourel 1997).

As a function of colour, the white and turquoise blue glazes have close chemical compositions: they are alkali-lead containing glazes, opacified with cassiterite (from

1.7 to 11.1 % of SnO<sub>2</sub>). Except from the presence of copper (from 1 to 2 % of CuO) which gives the turquoise blue colour, there is no obvious discrimination between the chemical compositions of these two glazes. The dark blue glazes are very different from the others: they contain alkali without any lead. Thus the alkali character is stronger. The dark blue colour is provoked by the presence of cobalt (from 0.4 to 0.6 % of CoO). The high amount of arsenic in the Iranian dark blue glazes comes from the cobaltiferous ore that is very probably a local one (Gratuze et al. 1996; Porter 2000).

These results corroborate Abu'l Qasim's treatise on ceramics as it describes how to obtain two kinds of frits: the first one, called *jawhar*, is a soda frit obtained from quartz and soda, which were melted and quenched in water; the second one contains soda-lead and it is obtained from talc and soda fired together and lead and tin oxide melted then quenched into water. Concerning the colours, Abu'l Qasim writes that "if the potters use one part of *lajvard*, [which is a cobalt ore] to forty parts of glaze frit it would give a transparent blue glaze". "To obtain a glowing white", they add tin to the frit. "If for every ten [or: two] parts of glaze frit they add (...) for every *man* of ground tin ten *dirhams* of ground roasted cooper", they obtain an opaque turquoise blue colour (Allan 1973).

The analytical results corroborate the 14<sup>th</sup> c. written source.

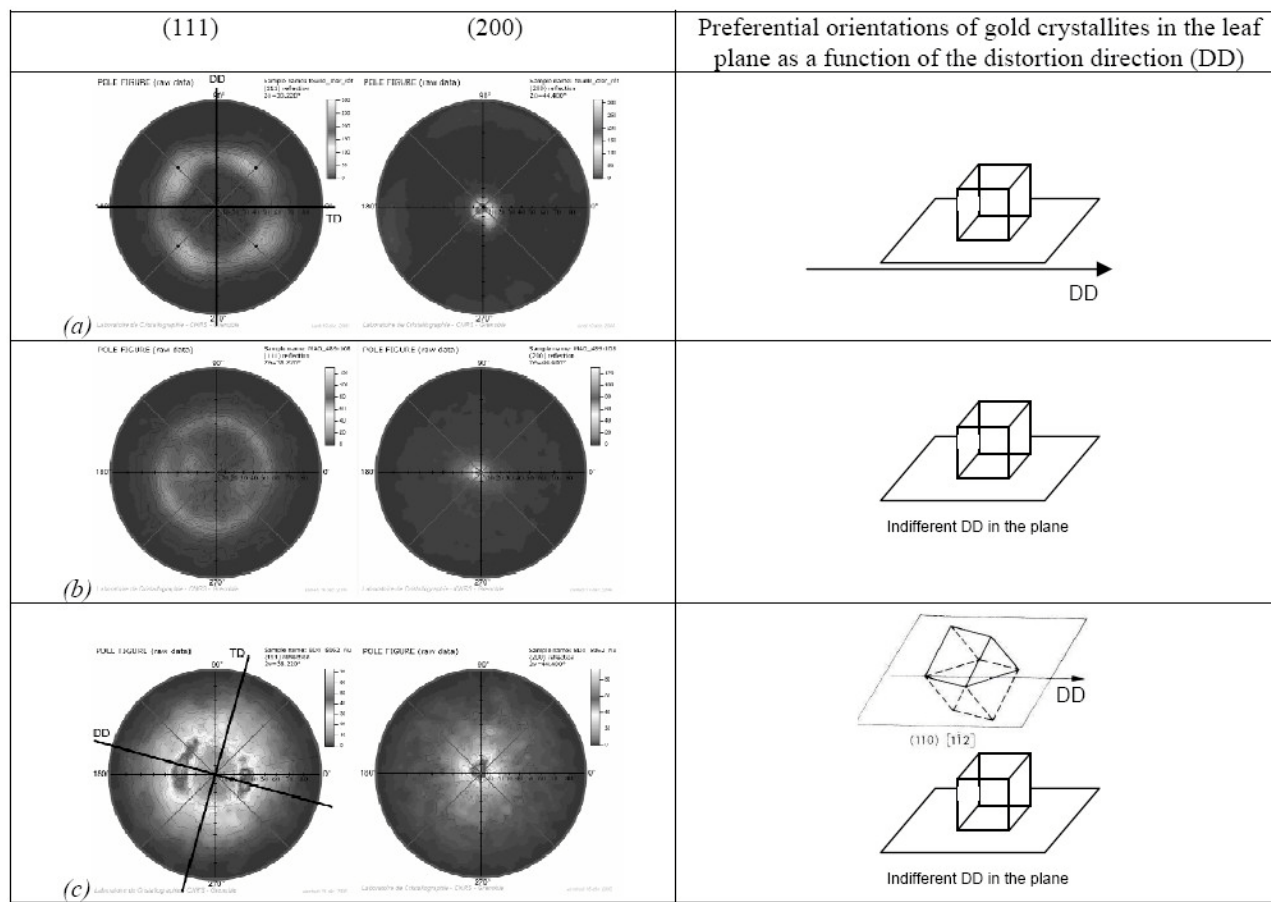


**Fig. 4** (a) Modern gold leaf (FREBA) – (111) and (200) pole figures. The texture is close to a cubic one whose ideal pole figures are indicated by the black dots ( $\bullet$ ). (b) Iran – 12<sup>th</sup>-13<sup>th</sup> c. – (111) and (200) pole figures of gold decorations, characteristic of a (200) fibre texture. (c) Central Asia – 14<sup>th</sup>-15<sup>th</sup> c. – (111) and (200) pole figures of Timurid gold leaf showing the coexistence of a rolled-brass-type and a (200) fibre textures. The distortion direction (DD) can be determined on the (111) pole figure, as well as the transverse direction (TD).

### The gold-leaf decorations

**Observations** In 12<sup>th</sup>-13<sup>th</sup> c. Iran architectural tiles with gold leaf are moulded and glazed. Vessels can be separated in three types of gold decorations: gold embellishments, gilded *barbotine* decorations and gilded central patterns (Pacheco 2007). In 14<sup>th</sup>-15<sup>th</sup> c. Central Asia there is no gold-leaf decoration on glazed vessels but it is widely used on architectural tiles (Pope 1939, Golombek et al. 1996). Only one type of gold decoration has been observed: central gilded patterns.

The observations of the latter patterns at different scales, as illustrated in Fig. 3, showed that the gold leaf is locally covered by the red outline that is always present on every sherd. The black decoration sometimes comes above the red pattern and it happens that the coloured glazes cover not only the red outline but also the gold leaf itself. These observations lead to establish the following *chaîne opératoire*:

- 1) Making of the clay and possible firing
- 2) Affixing of the glazing mixture
- 3) Firing
- 4) Affixing of the gold leaves (on a pattern probably obtained with a pouncing drawing)
- 5) Red outline
- 6) Black decoration
- 7) Affixing of the coloured glazing mixtures in the spaces delimited by the red and black decorations
- 8) Firing

In Abu'l Qasim's treatise (1301), the first step the author describes is the preparation of the gold leaves: "They hammer (...) gold into 24 sheets putting paper covered with plaster between them" (Allan 1973).

**Table 5** Chemical compositions and thicknesses of the layers composing the virtual target for the SIMNRA simulation of the RBS spectrum obtained on the ancient gold decoration and represented in figure 5. The roughness of the sample is taken into account with the FWHM (Full Width at Half Maximum) and the standard deviation is given by the formula  $FWHM = 2.35 \sigma$  (Mayer, 2006; Pacheco, 2007).

Layer	Elementary composition (atomic %)							Equivalent thickness ( $10^{15}$ at.cm <sup>-2</sup> )	FWHM ( $10^{15}$ at.cm <sup>-2</sup> )	$\sigma$ ( $10^{15}$ at.cm <sup>-2</sup> )
	Au	Ag	Si	O	Pb	Sn	Ca			
1	60	5	15	20				26000	10000	4450
2			52.4	39.3	0.8	2.5	5	substrate		

This is the description of the mechanical treatment gold undergoes, the forming being achieved by a bi-directional plastic distortion, as the gold beating process known from Ancient Egypt until nowadays (Nicholson 1979).

Then, “they cut [the gold leaves] carefully with scissors and stick them with a pen onto the vessels with dissolved glue and smooth them with cotton” (Allan 1973). The adhesion of gold on glass is brought about by unidentified glue. According to Abu’l Qasim, the next step is then to prepare the red mixture, to embellish it and then the black one.

Finally, “each of these [decorated ceramics] is (...) fired from morning till night at a low heat” (Allan 1973). The final necessary thermal treatment ends the process.

The process that has been established by surface observations corroborates the ancient process described by a reliable witness.

*Chemical compositions of the gold leaves* The chemical compositions of the gold leaves are given in **Table 4**.

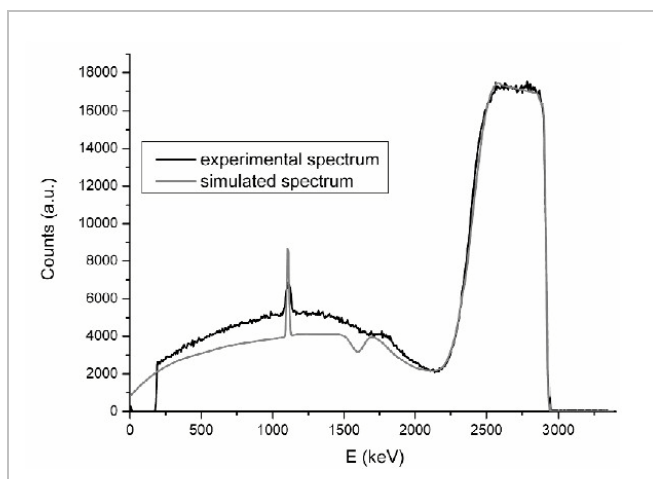


**Fig. 5** Central Asia – 14th-15th c. Experimental and SIMNRA-simulated RBS spectra obtained on an ancient gold decoration under a 3-MeV proton beam. Roughness has been taken into account and the resulting simulated spectrum fits the experimental one. The arrow indicates the back edge of gold.

The very low rates of silver and copper seem to indicate that gold is not alloyed and these elements may come from the auriferous ore itself (Guerra & Calligaro 2004).

*Texture of the gold leaves* The XRD pole figures of a modern gold leaf (FREBA enterprise), formed by rolling then by traditional beating, are determined and comparable to the literature (Kitagawa & Tanimura 1986).

The authors have showed the evolution of the pole figures of gold during the forming of the gold leaves: a gold alloy containing 4.90 % Ag and 0.66 % Cu, is rolled up to a 40  $\mu$ m thickness. The pole figures reveal a rolled-brass-type texture. Then the rolled gold sheets are beaten to a thickness of 0.1  $\mu$ m. At the end of the process the pole figures are characteristic of a (200) fibre texture.

The pole figures determined on the modern gold leaf (Fig. 4a) are characteristic of a cubic texture. The ancient gold decorations present distinct pole figures for the different corpuses: the Iranian gold leaf shows a perfect (200) fibre texture (Fig. 4b) whereas the Timurid sherd seems to present a (111) pole figure characteristic of a rolled-brass texture and a (200) fibre texture. The coexistence of both of these orientations makes us conclude that the Timurid gold leaves underwent a unidirectional plastic distortion and that the (200) orientation may be due to a bidirectional beating that has not been achieved, preventing the traces of the previous distortion from being completely erased. Nevertheless, it must not be forgotten that these decorations did undergo firing and that the existence of such orientations might be a consequence of the thermal treatment.

*Thickness of the gold leaves* A RBS spectrum obtained on ancient gold decoration is shown in **Fig. 5**.

The composition and parameters of the virtual target used for the SIMNRA simulation are given in **Table 5**. In Figure 5 the front edge at 2900 keV corresponds to the energy of the particles backscattered by gold atoms at the surface of the target. The deeper the gold atoms are, the lower the energy is. Thus, the width of the peak is directly correlated to the thickness of the gold leaf.

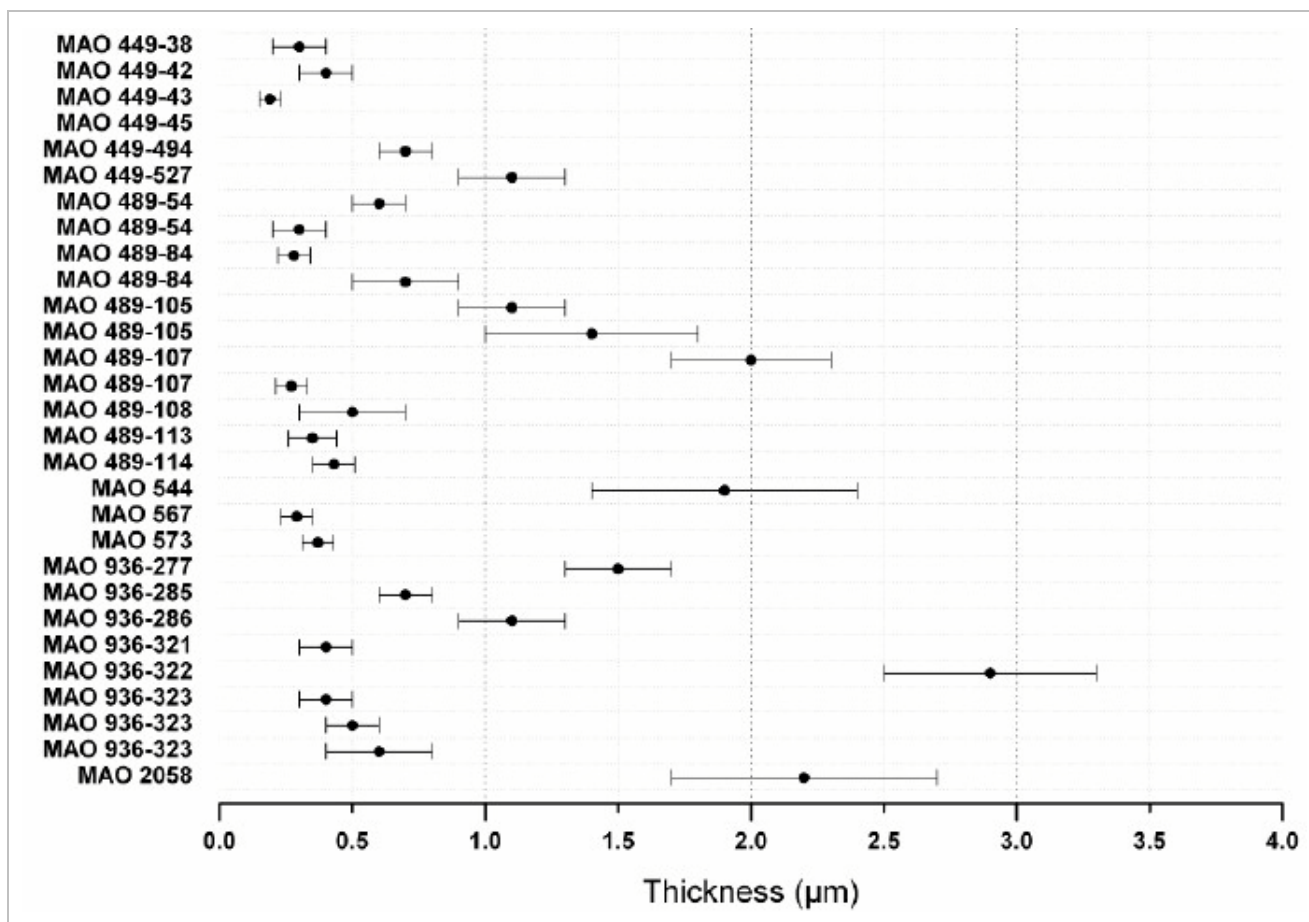


**Fig. 6** Iran – 12<sup>th</sup>-13<sup>th</sup> c. Comparison of the estimated thicknesses determined from the RBS simulations of the spectra obtained under a 3-MeV proton beam.

The back edge, indicated by the arrow in **Fig. 5**, is characteristic of the gold/glaze interface. Such a profile is characteristic of a gold concentration gradient in the glaze at the interface or of a rough surface or of the combination of both phenomena. As the roughness is not negligible (*Pacheco 2007*) it is taken into account in order to obtain a simulated spectrum that fits well the experimental one considering the distribution of the thickness as a gamma function. The FWHM of the gamma function is given in **Table 5** and the standard deviation  $\sigma$  is calculated as:  $\text{FWHM} = 2.35 \sigma$  (*Mayer 2006*).

In the illustrated case the thickness of the gold leaf corresponding to the first layer of the virtual target is estimated calculating the weighted average of gold and silver with the following values: Au:  $M_{\text{Au}} = 196.97 \text{ g.mol}^{-1}$ ;  $10^{15} \text{ at.cm}^{-2} = 0.1694 \text{ nm}$ ; Ag:  $M_{\text{Ag}} = 107.87 \text{ g.mol}^{-1}$ ;  $10^{15} \text{ at.cm}^{-2} = 0.1711 \text{ nm}$ . Then, the thickness is:  $26000 \times (0.6 \times 0.1694 + 0.05 \times 0.1711) = 2865 \text{ nm}$ . Taking the  $\sigma$  standard deviation into account the thickness of the gold leaf is  $2.9 \pm 0.5 \mu\text{m}$ .

Two other Timurid gold decorations have been through RBS analyses and the estimated thicknesses are:  $0.5 \pm 0.1 \mu\text{m}$  and  $1.3 \pm 0.4 \mu\text{m}$ . If the number of analyses prevents from a statistical study of the thickness distribution in the Timurid corpus it can, nevertheless be noticed that only one sherd presents a gold leaf decoration with a thickness inferior to  $1 \mu\text{m}$ .

Concerning the Iranian fragments 28 different thickness values could have been estimated in the same way. They are represented in **Fig. 6** and it can be determined that the average of the thickness is  $0.7 \mu\text{m}$  and the median value is  $0.5 \mu\text{m}$ . About 68 % of the thicknesses are lower than  $1 \mu\text{m}$ .

## CONCLUSIONS AND PERSPECTIVES

To the question “is gold-leaf decoration commonly used in 14<sup>th</sup>-15<sup>th</sup> c. Central Asia a *Persian tradition*?”, one can say it is. The ceramic bodies are not similar (only stoneware in 12<sup>th</sup>-13<sup>th</sup> c. Iran and mainly earthenware for the Timurid sherds), probably because clay is easier and

faster to shape than grounded quartz to rapidly provide tiles in furtherance of Timur's wish to settle his power. The glazes seem to be very similar in the two corpuses, corroborating Abu'l Qasim's recipes. The *chaîne opératoire* of the gold-leaf decorations is the same for the central gilded patterns in both corpuses and in the ancient treatise.

Concerning the interactions between the potters' and gold beaters' craft societies it can be said that the Iranian gold leaves were formed by bidirectional distortion from the XRD pole figure and are very thin regarding the RBS results. Only a master knowing the know-how could have obtained such a material meaning that in 12<sup>th</sup>-13<sup>th</sup> c. Iran potters took the gold leaves from gold beaters. In Timurid Central Asia this interaction between the craft societies is not so obvious: the XRD pole figures indicate that the gold leaves underwent a unidirectional plastic distortion and the (200) fibre direction may be due to an insufficient beating. The gold leaves seem to be thicker from the first RBS results. Several hypotheses can be raised: first, interactions existed between the societies but the gold beating was not achieved for unknown reasons (lack of time, overabundance of gold as a raw material, voluntary wish to make thicker foils for ceramics dedicated to architecture thus exposed to climatic conditions); then, the absence of such exchange – or even of the gold beaters themselves – can be envisaged, making the potters themselves form the gold leaves they needed without mastering the know-how.

In the future more RBS spectra will be acquired on the Central Asian corpus in order to statistically study the distribution of the thickness of the Timurid gold leaves. The effect of thermal treatment on the pole figures of a rolled and/or beaten not alloyed gold leaf will also be investigated.

#### ACKNOWLEDGEMENT

The authors would like to thank Mr N. Khushvaktov, curator of the Amir Timur Museum in Shakhriyabz (Uzbekistan), for giving the opportunity to study precious Timurid objects coming from the collections; Mr. J. Salomon and Mr. L. Pichon and all the AGLAE team for their helpful suggestions; Mr. L. Ortega for his help with the texture goniometre; and the French ANR (Agence Nationale de la Recherche) for giving the funds to the DORAI programme.

#### REFERENCES

- ALLAN, J. W. (1973): *Iran* vol.11:111-120.
- BLAIR, S. & BLOOM, J. M. (1994): *The Art and Architecture of Islam 1250-1800*. Yale University Press - Pelican History of Art.
- GOLOMBEK, L., MASON, R. B. & BAILEY, G. (1996): *Tamerlane's Tableware: a new approach to the Chinoiserie Ceramics of Fifteenth and Sixteenth Century Iran*. Mazda Press, Costa Mesa, and Royal Ontario Museum, Toronto.
- GRATUZE, B., SOULIER, I., BLET, M. & VALLAURI, L. (1996): *Revue d'Archéométrie* vol. 20 : 77-94.
- GUERRA, M. F. & CALLIGARO, T. (2004): *Journal of Archaeological Science* vol.31 : 1199-1208.
- KEHREN, L. (1978): *Tamerlan*. Paris, Payot, éd. de la Baconnière.
- KITAGAWA, K. & TANIMURA, K. (1986): *Scripta Metallurgica* vol.20: 1511-1514.
- LEROI-GOURHAN, A. (1945): *Milieu et techniques*. Albin Michel, Paris.
- MAYER, M. (2006): *SIMNRA user's guide*. [www.rzg.mpg.de/~mam/](http://www.rzg.mpg.de/~mam/).
- NICHOLSON, E. (1979): *Gold Bulletin* vol. 12(4): 161-166.
- PACHECO C., CHAPOULIE, R., DOORYHEE, E. & GOUDEAU, P. (2007): *Zeitschrift für Kristallographie Supplement* vol.26: 317-323.
- PACHECO, C. (2007): *Etude de films d'or sur matière vitreuse - Application à la céramique glaçurée islamique médiévale - Asie Centrale XIV<sup>e</sup>-XV<sup>e</sup> s. - Iran XII<sup>e</sup>-XIII<sup>e</sup> s.*, PhD thesis, Université Michel de Montaigne Bordeaux 3.
- PERNOT, M. (2006): *Cahiers d'Epistémé* vol.1: 7-25.
- POPE, A.U. (1939): *A survey of Persian art* vol. 4: 1541-1666.
- PORTER, V. (1995): *Islamic tiles*. London, The British Museum Press.
- PORTER, Y. (2000): *TAOCI - Revue annuelle de la Société Française d'Etude de la Céramique Orientale* vol. 1: 5-14.
- STERPENICH, J. & LIBOUREL, G. (1997): *Technè* vol. 6: 70-78.

